

## Synthesis and Characterization of a Nitroxide–Semiquinone Biradical

David A. Shultz\* and Gary T. Farmer

Department of Chemistry, North Carolina State University, Raleigh, North Carolina 27695-8204

Received March 26, 1998

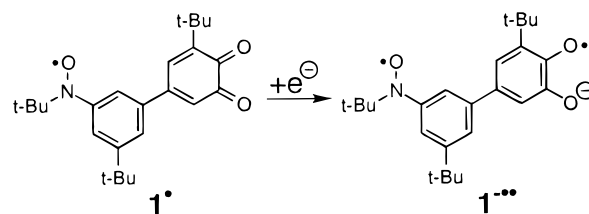
The synthesis and characterization of an anion biradical,  $1^{\bullet-}$ , composed of semiquinone and nitroxide functionalities is described. The biradical was prepared by reduction of the nitroxide–orthoquinone precursor using both electrochemical and chemical methods. The zero-field-splitting parameter,  $|D/hc|$ , for  $1^{\bullet-}$  is consistent with the proposed electronic structure, based on a comparison to  $|D/hc|$  of related biradicals. Finally, the results of variable-temperature EPR spectroscopy are in agreement with ferromagnetic (high-spin) coupling of the two unpaired electrons through the *m*-phenylene group.

Transition metal complexes of paramagnetic ligands constitute a significant portion of molecule-based magnets and are useful for studying structure–property relationships in exchange-coupled species in general. Many such materials feature metal–nitroxide complexes, metal–nitronyl nitroxide complexes, or metal–iminonitroxide complexes as the main structural element.<sup>1</sup> We are interested in using semiquinones as paramagnetic ligands to create extended solids, and we prepared a few bis-semiquinone ligands for this purpose.<sup>2,3</sup> However, it

occurred to us that interesting solids might be prepared from a single ligand having both semiquinone and nitroxide functionalities. Since semiquinone often coordinates metal ions through chelation,<sup>1q,u</sup> whereas the nitroxide group is monodentate,<sup>1a–p</sup> extended solids prepared from a mixed semiquinone–nitroxide ligand could yield unique structural and magnetic properties that are difficult to attain using a ligand having a single coordination mode. As the first step in preparing such materials, we report the synthesis and characterization of a nitroxide–semiquinone molecule,  $1^{\bullet}$ , prepared by reduction of monoradical  $1^{\bullet}$ .

(1) For papers on nitroxide complexes, see the following: (a) Caneschi, A.; Gatteschi, D.; Sessoli, R.; Rey, P. *Acc. Chem. Res.* **1989**, *22*, 392. (b) Caneschi, A.; Gatteschi, D.; Rey, P.; Sessoli, R. *Chem. Mater.* **1992**, *4*, 204. (c) Gatteschi, D.; Sessoli, R. *J. Magn. Magn. Mater.* **1992**, *104*, 2092. (d) Stumpf, H. O.; Ouahab, L.; Pei, Y.; Grandjean, D.; Kahn, O. *Science* **1993**, *261*, 447. (e) Gatteschi, D. *Adv. Mater.* **1994**, *6*, 635. (f) Luneau, D.; Laugier, J.; Rey, P.; Ulrich, G.; Ziessel, R.; Legoll, P.; Drillon, M. *J. Chem. Soc., Chem. Commun.* **1994**, 741. (g) Kitano, M.; Koga, N.; Iwamura, H. *J. Chem. Soc., Chem. Commun.* **1994**, 447. (h) Kitano, M.; Ishimaru, Y.; Inoue, K.; Koga, N.; Iwamura, H. *Inorg. Chem.* **1994**, *33*, 6012. (i) de Panthou, F. L.; Belorizky, E.; Calemczuk, R.; Luneau, D.; Marcenat, C.; Ressouche, E.; Turek, P.; Rey, P. *J. Am. Chem. Soc.* **1995**, *117*, 11247. (j) Inoue, K.; Hayamizu, T.; Iwamura, H.; Hashizume, D.; Ohashi, Y. *J. Am. Chem. Soc.* **1996**, *118*, 1803. (k) Pei, Y.; Kahn, O.; Ouahab, L. *Inorg. Chem.* **1996**, *35*, 193. (l) Iwamura, H.; Inoue, K.; Hayamizu, T. *Pure Appl. Chem.* **1996**, *68*, 243. (m) Ottaviani, M. F.; Turro, C.; Turro, N. J.; Bossman, S. J.; Tomlalia, D. *J. Phys. Chem.* **1996**, *100*, 13667. (n) Sokolowsky, A.; Bothe, E.; Bill, E.; Weyhermueller, T.; Wieghardt, K. *Chem. Commun.* **1996**, 6, 1671. (o) Nakatsujii, S.; Anzai, H. *J. Mater. Chem.* **1997**, *7*, 2161. (p) Fegy, K.; Luneau, D.; Ohm, T.; Paulsen, C.; Rey, P. *Angew. Chem., Int. Ed. Engl.* **1998**, *37*, 1270; for some interesting non-nitroxide paramagnetic ligand–metal complexes, see the following: (q) Pierpont, C. G.; Buchanan, R. M. *Coord. Chem. Rev.* **1981**, *38*, 45. (r) Gans, P.; Buisson, G.; Duee, E.; Marchon, J. C.; Erlor, B. S.; Scholz, W. F.; Reed, C. A. *J. Am. Chem. Soc.* **1986**, *108*, 1223. (s) Miller, J. S.; Calabrese, J. C.; McLean, R. S.; Epstein, A. J. *Adv. Mater.* **1992**, *4*, 498. (t) Gatteschi, D.; Dei, A. *Inorg. Chim. Acta* **1992**, *198–200*, 813. (u) Pierpont, C. G.; Lange, C. W. *Prog. Inorg. Chem.* **1994**, *41*, 331. (v) Adams, D. M.; Li, B.; Simon, J. D.; Hendrickson, D. N. *Angew. Chem., Int. Ed. Engl.* **1995**, *34*, 1481. (w) Hintermaier, F.; Sünkel, K.; Volodarsky, L. B.; Beck, W. *Inorg. Chem.* **1996**, *35*, 5500. (x) Zhao, H.; Heintz, R. A.; Dunbar, K. R.; Rogers, R. D. *J. Am. Chem. Soc.* **1996**, *118*, 12844; for general texts on molecular magnetism, see the following: (y) Gatteschi, D. *Molecular Magnetic Materials*; Kluwer Academic Publishers: Amsterdam, 1991. (z) Kahn, O. *Molecular Magnetism*; VCH: New York, 1993. (aa) *Molecular Magnetism: From Molecular Assemblies to the Devices*; Coronado, E., Delhaes, P., Gatteschi, D., Miller, J. S., Eds.; Kluwer Academic Publishers: Dordrecht, The Netherlands, 1996; Vol. 321. (bb) *Molecule-Based Magnetic Materials. Theory, Technique, and Applications*; Turnbull, M. M., Sugimoto, T., Thompson, L. K., Eds.; ACS Symposium Series 644 American Chemical Society: Washington, DC, 1996.

(2) Shultz, D. A.; Boal, A. K.; Driscoll, D. J.; Farmer, G. T.; Hollomon, M. G.; Kitchin, J. R.; Miller, D. B.; Tew, G. N. *Mol. Cryst. Liq. Cryst.* **1997**, *305*, 303.



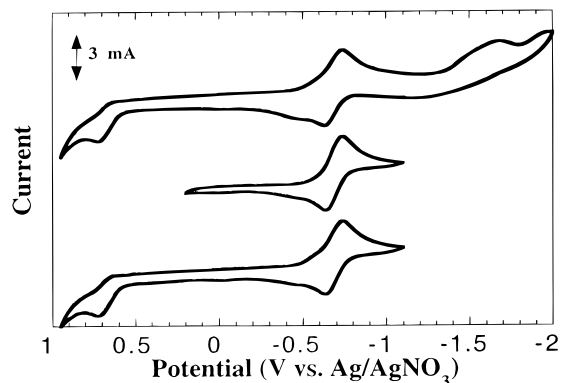
The synthesis of radical  $1^{\bullet}$  is shown below. Boronic acid  $2^2$  was used as a coupling partner in a Suzuki coupling reaction with bromide  $3^4$  to give  $4$  in good yield. Selective deprotection of  $4$  with  $\text{BBr}_3$  gave the corresponding catechol in excellent yield, followed by TBS-removal using tetra-*n*-butylammonium fluoride. The catechol–hydroxylamine was immediately oxidized with Fetizon's reagent<sup>5</sup> to provide quinone–nitroxide  $1^{\bullet}$  in high yield. This oxidation was dramatically faster than those of other catechols with which we have dealt. In fact, the oxidation that yields  $1^{\bullet}$  was typically complete within thirty minutes as opposed to a reaction time of 12 h required for completion of a typical catechol oxidation. Longer reaction times resulted in the formation of inseparable mixtures of oxidation products derived from  $1^{\bullet}$ .<sup>6</sup> Compound  $1^{\bullet}$  exhibits three infrared signals from 1620 to 1680  $\text{cm}^{-1}$  providing conclusive evidence for the orthoquinone functionality of  $1^{\bullet}$ .

Figure 1 shows cyclic voltammograms of  $1^{\bullet}$ . The reversible feature near  $-0.7$  V is characteristic of the

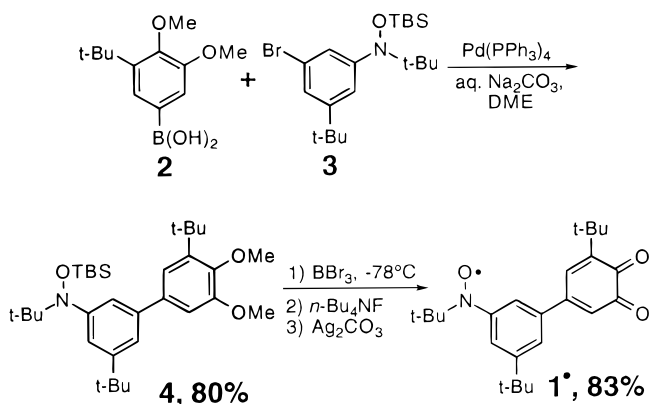
(3) Shultz, D. A.; Boal, A. K.; Driscoll, D. J.; Kitchin, J. R.; Tew, G. N. *J. Org. Chem.* **1995**, *60*, 3578.

(4) Ishida, T.; Iwamura, H. *J. Am. Chem. Soc.* **1991**, *113*, 4238.

(5) Balogh, V.; Fetizon, M.; Golfier, M. *J. Org. Chem.* **1971**, *36*, 1339.



**Figure 1.** Cyclic voltammograms of **1\*** in THF (ca. 1 mmol) with tetra-*n*-butylammonium hexafluorophosphate (ca. 100 mmol) as supporting electrolyte. Scan rates = 200 mV/s.



orthoquinone  $\leftrightarrow$  semiquinone redox reaction, while the irreversible waves between  $-1.4$  V and  $-1.8$  V are typical for the semiquinone  $\leftrightarrow$  catecholate couple<sup>3,7</sup> and the nitroxide radical  $\leftrightarrow$  nitroxide anion couple.<sup>8</sup>

The final cyclic voltammetric feature is the irreversible couple near  $+0.6$  V, which we attribute to the nitroxide radical  $\leftrightarrow$  nitronium cation couple.<sup>8</sup> For other aryl-*tert*-butylnitroxides we have prepared, a reversible wave is observed in this region. At present, we cannot explain why this nitroxide displays irreversible behavior; however, it is consistent with the destructive  $\text{Ag}_2\text{CO}_3$ -promoted chemical oxidations observed at reaction times exceeding 1 h.

The EPR spectrum of **1\*** as a solution in THF recorded at 298 K consists of a triplet of apparent quartets. Hyperfine couplings obtained by spectral simulation<sup>9</sup> are:  $a_N = 12.53$  G;  $a_H = 1.80$  G (3H) as given in Table 1. As expected, hyperfine couplings are not observed for quinone-ring protons since the quinone is *meta* to the nitroxide, and the unpaired electron cannot be resonance delocalized into the quinone.

The biradical  $n\text{-Bu}_4\text{N}^+\text{1}^{2-}$  was prepared by controlled potential coulometry at  $-1.1$  V vs  $\text{Ag}/\text{AgNO}_3$  of **1\*** as a

(6) Extended reaction times gave several compounds having anhydride-type C=O stretches ( $1717$ ,  $1767$   $\text{cm}^{-1}$ ) characteristic of intradiol cleavage products. For more information about intradiol cleavage, see refs 1q and 1u.

(7) Stallings, M. D.; Morrison, M. M.; Sawyer, D. T. *Inorg. Chem.* **1981**, *20*, 2655.

(8) Shultz, D. A.; Boal, A. K. Unpublished results.

(9) Fluid solution EPR spectra were simulated using the EPR Calculations for MS-Windows NT/95, Version 0.96, Public EPR Software Tools, National Institute of Environmental Health Sciences, National Institutes of Health, Research Triangle Park, NC.; Dave Duling, 1996. The correlation coefficient for the simulation is  $R = 0.994$ .

**Table 1.** EPR Spectral Data for Nitroxide **1\*** and Biradical Anion **1<sup>2-</sup>**<sup>a</sup>

compound	$a_N$ (Gauss)	$a_H$ (Gauss)	$ D/hc $ ( $\text{cm}^{-1}$ )	$ E/hc $ ( $\text{cm}^{-1}$ )
<b>1*</b>	12.53	1.80	—	—
$\text{Na}^+\text{1}^{2-}$ (PMDTA)	—	—	$\approx 0.0084^b$	$c$

<sup>a</sup> Hyperfine coupling constants (hfcc) estimated by simulation<sup>9</sup> of experimental spectrum. <sup>b</sup> Zero-field-splitting parameter estimated as one-half the difference between the  $Z_1$  and  $Z_2$  transitions, see text. <sup>c</sup>  $|E/hc|$  could not be estimated due to spectral complexity in the  $X/Y$  regions of the  $\Delta m_s = 1$  transitions.

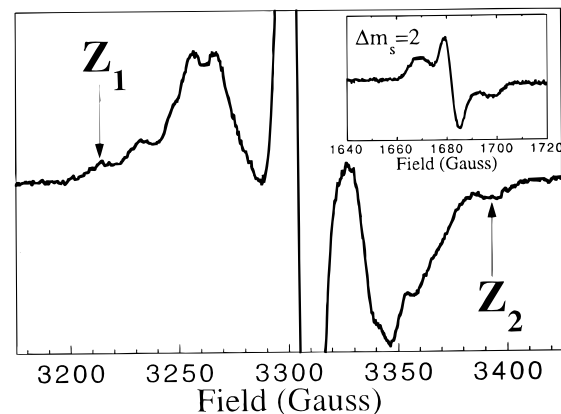
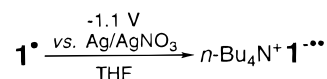


**Figure 2.** X-band EPR spectrum of biradical  $\text{Na}^+\text{1}^{2-}$ (PMDTA) as a frozen solution in THF at 77 K. Arrows indicate the spectral features used to estimate the zero-field-splitting parameter,  $D$ . Inset:  $\Delta m_s = 2$  transition.

solution in THF in a standard two-compartment cell, with tetra-*n*-butylammonium hexafluorophosphate as supporting electrolyte.



Alternatively,  $\text{Na}^+\text{1}^{2-}$ (PMDTA) (PMDTA = pentamethyldiethylenetriamine) was prepared by reduction of **1\*** with  $\text{Na}^+\text{DBSQ}^{\cdot-}$ (PMDTA) ( $\text{DBSQ}^{\cdot-} = 3,5\text{-di-}t\text{-butylsemiquinone}$ ). The triamine, PMDTA, is effective at inhibiting aggregation which can result in additional spectral features.<sup>10</sup> Frozen solution EPR spectral features of **1<sup>2-</sup>** obtained by electrochemical reduction and chemical reduction were similar.<sup>11</sup>

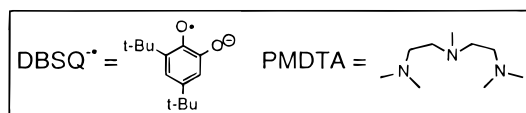
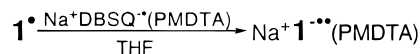


Figure 2 shows the frozen solution EPR spectrum of  $\text{Na}^+\text{1}^{2-}$ (PMDTA) recorded at 77 K. The spectrum is typical for a randomly oriented triplet biradical.<sup>12,13</sup> Also present is a  $\Delta m_s = 2$  transition, the signature of a high-

(10) Shultz, D. A.; Boal, A. K.; Campbell, N. P. *Inorg. Chem.* **1998**, *37*, 1540.

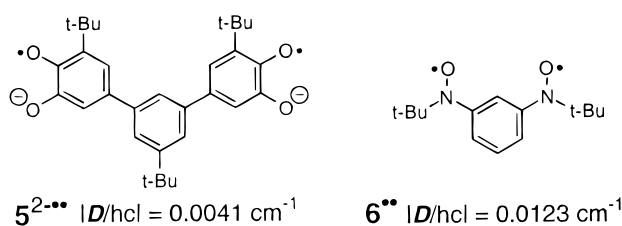
(11) See Supporting Information for EPR spectrum from bulk electrolysis.

(12) Wasserman, E.; Snyder, L. C.; Yager, W. A. *J. Chem. Phys.* **1964**, *41*, 1763.

(13) Wertz, J. E.; Bolton, J. R. *Electron Spin Resonance*; Chapman and Hall: New York, 1986.

spin state.<sup>14</sup> Anisotropic N-hyperfine structure is visible in the  $\Delta m_s = 2$  transition with nominal  $A_{N,\parallel}$  and  $A_{N,\perp}$  values one-half those of the corresponding N-hyperfine couplings of the monoradical **1**<sup>•</sup>, consistent with  $|J| \gg |A|$  for Na<sup>+</sup>**1**<sup>••</sup>(PMDTA).<sup>15</sup> Spectral features in the  $\Delta m_s = 1$  region are unaffected by temperature changes from 8 to 77 K, suggesting that conformers with dramatically different structures and therefore different zero-field splitting parameters are unlikely.<sup>16</sup>

The zero-field-splitting parameter,  $|D/hc|$ , estimated from spectral features (one-half the difference between the  $Z_2$  and  $Z_1$  transitions:  $(Z_2 - Z_1)/2$ ) is given in Table 1. We are unable to estimate  $|E/hc|$  due to the large number of lines in the X/Y regions of the spectrum (ca. 3250 and 3350 G). We believe some of these features are N-hyperfine lines such as those observed in biradical **6**<sup>••</sup>.<sup>17,18a</sup> Consistent with electronic structure, the  $D$ -value of Na<sup>+</sup>**1**<sup>••</sup>(PMDTA), 0.0084 cm<sup>-1</sup>, is quite close to the average (0.0082 cm<sup>-1</sup>) of biradicals **5**<sup>2-••3</sup> and **6**<sup>••</sup>.<sup>18b</sup>



A plot of the temperature dependence of the EPR signal intensity (a Curie plot) can sometimes be useful for determining the exchange coupling constant,  $J$ , and therefore the singlet–triplet energy gap ( $2J$ ).<sup>19,20</sup> If the signal varies linearly when plotted vs inverse absolute temperature, then the species is either a ground-state triplet, or there is a singlet–triplet degeneracy. However, if there is significant curvature in the Curie plot and intensity decreases at lower temperatures, then  $J$  can be estimated from a multiparameter fit, and the biradical is a ground-state singlet. Figure 3 shows the Curie plot for the doubly integrated  $\Delta m_s = 2$  signal of Na<sup>+</sup>**1**<sup>••</sup>(PMDTA) in THF. The linear relationship between signal intensity and inverse temperature is characteristic of a triplet ground-state, consistent with high-spin coupling enforced by the *m*-phenylene moiety.<sup>21</sup>

In summary, we synthesized a novel biradical designed to differentially bind two metal ions. Cyclic voltammetry and EPR spectroscopy were used to characterize the biradical and its monoradical precursor. Biradical **1**<sup>••</sup> exhibits a zero-field-splitting parameter,  $|D/hc|$ , that is

(14) Dougherty, D. A. In *Kinetics and Spectroscopy of Carbenes and Biradicals*; Platz, M. S., Ed.; Plenum Press: New York, 1990.

(15) The  $A$ -values obtained from spectral simulation (or from inspection) for a biradical are actually  $A/2$  when  $|J| \gg |a|$ , see ref 13, or Atherton, N. M. *Principles of Electron Spin Resonance*; Ellis Horwood PTR Prentice Hall: New York, 1993.

(16) Shultz, D. A.; Boal, A. K.; Farmer, G. T. *J. Am. Chem. Soc.* **1997**, *119*, 3846.

(17) Calder, A.; Forrester, A. R.; James, P. G.; Luckhurst, G. R. *J. Am. Chem. Soc.* **1969**, *91*, 3724.

(18) (a) Of course, we cannot completely rule out that some of the spectral features of **1**<sup>••</sup> could be due to conformers with different zero-field-splitting parameters. (b) At least two conformations of **6**<sup>••</sup> were observed in frozen ethanol, one of which exhibited  $|D/hc| > 0.0123 \text{ cm}^{-1}$ .

(19) *The Chemistry of Quinonoid Compounds*; Berson, J. A., Ed.; John Wiley & Sons: New York, 1988; Vol. II.

(20) Berson, J. A. *Diradicals*; Wiley: New York, 1982.

(21) As noted in the text, this linear relationship is also consistent with  $J = 0$ ; however, this seems unlikely considering that the spectral features of the  $\Delta m_s = 2$  transition are consistent with  $|J| \gg |a|$ .

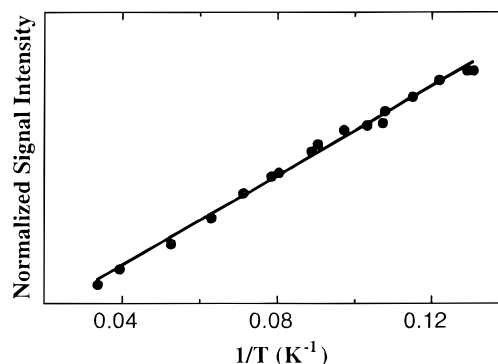


**Figure 3.** Curie plot for biradical Na<sup>+</sup>**1**<sup>••</sup>(PMDTA). The data points were collected between 8 and 30 K and represent normalized signal intensities obtained by double integration of the  $\Delta m_s = 2$  signals from two separate experiments. Linear fit (solid line) has a correlation coefficient of 0.997.

close to the average of those of the corresponding bis-semiquinone and bis-nitroxide. The results of variable-temperature EPR spectroscopy are consistent with ferromagnetic coupling of the two unpaired electrons through the *m*-phenylene group. The preparation of metal complexes of **1**<sup>••</sup> is underway and will be reported elsewhere.

## Experimental Section

**General.** Solvent distillations, synthetic procedures, and EPR sample preparation were carried out under an argon or nitrogen atmosphere. DME (anhydrous) and other chemicals were purchased from Aldrich Chemical Co. Trimethyl borate was dried over sodium and distilled prior to use. TBAF (1 M in THF) was degassed before use. THF was distilled from sodium benzophenone–ketyl prior to use, while CH<sub>2</sub>Cl<sub>2</sub> was distilled from CaH<sub>2</sub>. NMR spectra were recorded on a Varian 300 MHz spectrometer using deuteriochloroform as solvent and referenced to protiochloroform at 7.26 ppm for <sup>1</sup>H spectra and 77.2 ppm for <sup>13</sup>C spectra, or deuteriomethylene chloride referenced to protiomethylene chloride at 5.23 ppm for <sup>1</sup>H spectra and 54.0 ppm for <sup>13</sup>C spectra, or deuterioacetone referenced to protioacetone at 2.05 ppm for <sup>1</sup>H spectra and 30.0 ppm for <sup>13</sup>C spectra. Elemental analysis was performed by Atlantic Microlab, Inc, Norcross, GA. Electrochemical experiments were performed with a EG&G PAR Model 273 potentiostat. THF (anhydrous) solutions for electrochemistry were ca. 1 mM (voltammetry) or 2.5 mM (coulometry) in substrate and 100 mM in tetra-*n*-butylammonium hexafluorophosphate electrolyte. Pt disk and Pt wire served as the working and auxiliary electrodes, respectively, and the reference electrode was Ag/AgNO<sub>3</sub> in acetonitrile. Bulk electrolyses were performed using a standard “H-cell” equipped with Pt mesh working and counter electrodes and Ag/AgNO<sub>3</sub> in acetonitrile reference electrode. X-band EPR spectra were recorded on an IBM-Brüker E200SRC spectrometer fitted with an Oxford model 900 Cryostat. Frozen-solution EPR spectroscopy was performed on 2.5 mM solutions of **1**<sup>••</sup> in THF. Saturation experiments were performed to ensure that the concentration and gain/modulation settings gave signal responses that were a linear function of 1/attenuation.

**3,4-Dimethoxy-5,5'-di-*tert*-butyl-3'-[[*N*-*tert*-butyl-*N*(*tert*-butyl)dimethylsiloxy]amino]biphenyl (**4**).** 5-Bromo-3-*tert*-butylcatechol dimethyl ether<sup>2</sup> (1.5 g 5.49 mmol) was dissolved in dry THF (20 mL) and cooled to  $-78^\circ\text{C}$ . *tert*-Butyllithium (7.32 mL, 10.98 mmol) was added dropwise via a syringe over a 20 min period. After stirring 1 h, trimethyl borate (1.87 mL, 16.47 mmol) was added, and the reaction mixture was allowed to warm to room temperature. The reaction was stirred an additional 3 h, at which time the solvent and excess trimethyl borate were removed by bulb-to-bulb vacuum distillation. The resulting white paste was dissolved in DME (10 mL), and Pd-



(PPh<sub>3</sub>)<sub>4</sub> (254 mg, 0.22 mmol) and **3**<sup>4</sup> (2.00 g, 4.825 mmol) were added with argon purging, followed by stirring for 15 min. Aqueous Na<sub>2</sub>CO<sub>3</sub> (5.49 mL, 10.98 mmol) was added, and the mixture was refluxed overnight. After cooling, the reaction mixture was filtered through Celite, and the DME was removed using a rotoevaporator. The remaining material was dissolved in Et<sub>2</sub>O and washed with satd aqueous NaCl. The organic layer was dried over Na<sub>2</sub>SO<sub>4</sub>, concentrated, and purified by column chromatography (SiO<sub>2</sub>, 3% Et<sub>2</sub>O in petroleum ether) to yield 2.04 g of a white solid (80% yield): <sup>1</sup>H NMR (CH<sub>2</sub>Cl<sub>2</sub>, 300 MHz) δ: 7.27 (3H, bs), 7.09 (1H, d, *J* = 2.1 Hz), 7.01 (2H, d, *J* = 2.1 Hz), 3.90 (3H, s), 3.88 (3H, s), 1.41 (9H, s), 1.35 (9H, s), 1.12 (9H, s), 0.95 (9H, s), -0.08 (6H, bs); <sup>13</sup>C NMR (CDCl<sub>3</sub>, 75 MHz) δ: 153.52, 151.23, 150.53, 148.16, 143.47, 140.35, 137.08, 121.79, 121.29, 120.52, 118.07, 110.04, 61.01, 60.65, 56.07, 35.42, 34.89, 31.59, 30.79, 26.13, 18.21, -4.47. Anal. Calcd for C<sub>32</sub>H<sub>53</sub>NO<sub>3</sub>Si: C, 72.81; H, 10.12; N, 2.65. Found: C, 72.74; H, 10.21; N, 2.60.

**3,4-Dihydroxy-5,5'-di-*tert*-butyl-3'-[[*N*-*tert*-butyl-*N*-(*tert*-butyldimethylsiloxy)]amino]biphenyl (**4a**).** Biphenyl derivative **4** (100 mg, 0.19 mmol) was dissolved in dry CH<sub>2</sub>Cl<sub>2</sub> (5 mL) and cooled to -78 °C. BBr<sub>3</sub> (0.09 mL, 0.95 mmol) was added slowly via syringe, and the solution was stirred for 6 h at -78 °C. The reaction was then poured onto ice and an aqueous solution of NH<sub>4</sub>Cl and washed with a satd aqueous solution of NaCl. The organic layer was dried over Na<sub>2</sub>SO<sub>4</sub>, concentrated, and purified by chromatography using radial chromatography (SiO<sub>2</sub>, 1–20% Et<sub>2</sub>O in petroleum ether) to give 90 mg of a white solid (97% yield): <sup>1</sup>H NMR (CD<sub>2</sub>Cl<sub>2</sub>, 300 MHz) δ: 7.24 (2H, bs), 7.21 (1H, bs), 7.07 (1H, d, *J* = 1.86 Hz), 6.97 (1H, d, *J* = 1.86 Hz), 5.72 (1H, s), 5.09 (1H, s), 1.44 (9H, s), 1.33 (9H, s), 1.31 (9H, s), 0.93 (9H, s), -0.08 (6H, bs); <sup>13</sup>C NMR (CD<sub>2</sub>Cl<sub>2</sub>, 75 MHz) δ: 151.68, 151.11, 143.78, 143.48, 140.37, 137.13, 133.71, 121.80, 121.41, 120.62, 118.64, 112.32, 61.26, 35.27, 35.18, 31.72, 29.90, 26.60, 18.48, -4.33. IR (film from CH<sub>2</sub>Cl<sub>2</sub>): 3521 cm<sup>-1</sup>. HRMS (FAB) Calcd for C<sub>30</sub>H<sub>49</sub>NO<sub>3</sub>Si (M<sup>+</sup>): 499.3482. Found: 499.3489.

**3,4-Dimethoxy-5,5'-di-*tert*-butyl-3'-[[*N*-*tert*-butyl-*N*-hydroxyamino]biphenyl (**4b**).** Catechol **4a** (167 mg, 0.33 mmol) was dissolved in dry THF (5 mL) and cooled to 0 °C. Tetrabutylammonium fluoride (1.7 mL, 1 M in THF) was added via syringe, and the solution was allowed to warm to room temperature. The solution was stirred overnight and

then quenched with satd aqueous NH<sub>4</sub>Cl (1 mL). The solution was washed with satd aqueous NaCl, the organic layer was separated, dried over Na<sub>2</sub>SO<sub>4</sub>, and concentrated, and the residue was purified by chromatography using radial chromatography (SiO<sub>2</sub>, 10–30% Et<sub>2</sub>O in petroleum ether) to give 122 mg of a pink solid (95% yield): <sup>1</sup>H NMR ((CD<sub>3</sub>)<sub>2</sub>CO 300 MHz) δ: 9.00 (1H, bs), 7.60 (1H, bs), 7.25 (2H, s), 7.16 (1H, s), 7.00 (1H, s), 6.96 (1H, s), 1.41 (9H, s), 1.30 (9H, s), 1.12 (9H, s); <sup>13</sup>C NMR ((CD<sub>3</sub>)<sub>2</sub>CO, 75 MHz) δ: 151.96, 151.34, 146.08, 144.94, 141.98, 137.01, 133.59, 121.37, 120.85, 117.68, 112.89, 60.87, 35.73, 35.58, 32.18, 26.99; IR (film from CH<sub>2</sub>Cl<sub>2</sub>): 3242 cm<sup>-1</sup>. HRMS (FAB) Calcd for C<sub>24</sub>H<sub>36</sub>NO<sub>3</sub> (M + H)<sup>+</sup>: 386.2695. Found: 386.2693.

**3-*tert*-butyl-5-[3'-(*N*-*tert*-butyl-*N*-oxyamino)-5'-*tert*-butylphenyl]-1,2-benzoquinone (**1**).** Catechol–hydroxylamine **4b** (140 mg, 0.36 mmol) was dissolved in dry THF (20 mL), and Fetizon's reagent (Ag<sub>2</sub>CO<sub>3</sub> on Celite<sup>5</sup> ca. 50 wt %, 1 g) was added. After being stirred for 20 min, the mixture was filtered through a plug of Celite on a fritted funnel. The filtrate was concentrated and the residue purified by chromatography using radial chromatography (SiO<sub>2</sub>, 5–20% Et<sub>2</sub>O in petroleum ether as eluent) to give 125 mg of a brown/green solid (90% yield): IR (film from CH<sub>2</sub>Cl<sub>2</sub>): 1682, 1659, 1622 cm<sup>-1</sup>. Anal. Calcd for C<sub>24</sub>H<sub>32</sub>NO<sub>3</sub>: C, 75.36; H, 8.43; N, 3.66. Found: C, 75.11; H, 8.55; N, 3.55.

**Acknowledgment.** We thank the National Science Foundation (Grant CHE-9634878) for support of this work. D.A.S. also thanks the Camille and Henry Dreyfus Foundation for a Camille Dreyfus Teacher-Scholar Award. Mass spectra were obtained at the Mass Spectrometry Laboratory for Biotechnology. Partial funding for the Facility was obtained from the North Carolina Biotechnology Center and the National Science Foundation.

**Supporting Information Available:** Synthetic details and spectral data (24 pages). This material is contained in libraries on microfiche, immediately follows this article in the microfilm version of the journal, and can be ordered from the ACS; see any current masthead page for ordering information.

JO980562P